Locally grown $Cu(In,Ga)Se_2$ micro islands for concentrator solar cells

M. Schmid*[a,b], B. Heidmann[a,b], F. Ringleb[c], K. Eylers[c], O. Ernst[c], S. Andree[d], J. Bonse[d], T. Boeck[c], J. Krüger[d]

[a]University of Duisburg-Essen and CENIDE, Faculty of Physics, Lotharstr. 1, 47057 Duisburg, Germany; [b]Helmholtz-Zentrum Berlin für Materialien und Energie, Department Renewable Energy, Hahn-Meitner-Platz 1, 14109 Berlin, Germany; [c]Leibniz Institute for Crystal Growth, Max-Born-Straße 2, 12489 Berlin, Germany; [d]Bundesanstalt für Materialforschung und -prüfung, Unter den Eichen 87, 12205 Berlin, Germany

ABSTRACT

Light concentration opens up the path to enhanced material efficiency of solar cells via increased conversion efficiency and decreased material requirement. For true material saving, a fabrication method allowing local growth of high quality absorber material is essential. We present two scalable fs-laser based approaches for bottom-up growth of $Cu(In,Ga)Se_2$ micro islands utilizing either site-controlled assembly of In(,Ga) droplets on laser-patterned substrates during physical vapor deposition, or laser-induced forward transfer of (Cu,In,Ga) layers for local precursor arrangement. The $Cu(In,Ga)Se_2$ absorbers formed after selenization can deliver working solar devices showing efficiency enhancement under light concentration.

Keywords: local growth, self-assembly, fs-laser patterning, laser-induced forward transfer, chalcopyrite, $Cu(In,Ga)Se_2$, micro solar cell, light concentration

1. INTRODUCTION

The global energy demand is continuously increasing, urging further development of renewable energy sources. Solar energy currently holds a share of only few percent of the electricity production worldwide, although it has the potential - at least as far as available energy is concerned - of covering the total world energy demand [1]. Optimization of material usage and costs is a key to increase the deployment of the photovoltaics (PV) technology. In this respect, thin-film PV have brought an important step forward, as well as it has the exploitation of light concentration for further material reduction and efficiency enhancement. A combination of these two directions - thin film PV and light concentration - in the form of micro concentrator solar cells appears appealing, due to a compact module design related with improved heat dissipation as compared to large scale concentrating systems. Since $Cu(In,Ga)Se_2$ (CIGSe) solar cells have proven the highest stabilized record efficiency amongst the polycrystalline thin film devices, recently reaching 22.9% [2], we choose this material system for development of the micro concentrator concept.

CIGSe micro concentrator solar cells have attracted increasing attention over the last years. Proof-of-principle studies were carried out in top-down approaches based on micro cells defined by etching or shading of planar absorbers. In this way, Paire et al. could achieve an absolute efficiency increase of 5% at 475 suns for a 50 µm diameter micro cell defined by shading [3]. Similarly, Reinhold et al. reached 4.8% increase for point-shaped micro cells [4]. Lotter et al. obtained 22.5% efficiency, corresponding to a 4% increase at 77 suns, by selective etching of the front layers to define a 0.06 mm^2 micro cell [5]. By etching of the absorber itself, Sancho-Martinez et al. fabricated a 400 µm diameter micro cell which showed an efficiency enhancement of 3.2% absolute at 70x concentration [6]. Although these studies have revealed high potential for efficiency gain, they are missing the aspect of material saving. For this purpose, bottom-up approaches are studied that aim at local absorber growth. One method of selective growth is electrodeposition, based on which Duchatelet et al. fabricated line-shaped micro cells on corresponding Mo back contact lines [7]. In a similar approach, Sadewasser et al. deposited CIGSe micro cells in point openings of SiO_2 mask layers [8].

*martina.schmid@uni-due.de

Physics, Simulation, and Photonic Engineering of Photovoltaic Devices VII, edited by Alexandre Freundlich, Laurent Lombez, Masakazu Sugiyama, Proc. of SPIE Vol. 10527, 1052707
 · doi: 10.1117/12.2288253

Recently, we have demonstrated the local growth of $CuInSe_2$ (CISe) from indium islands, achieving opto-electronic material quality comparable to planar reference layers [9]. Furthermore, we have shown that laser-induced forward transfer (LIFT) of (Cu,In,Ga) precursor layers is also suitable for local fabrication of CIGSe micro absorbers in a sequential process [10]. In this paper, results from the two approaches are combined and extended for the study of resulting micro solar cells investigated at standard test conditions and under light concentration.

2. EXPERIMENTAL

The two fabrication approaches of local chalcopyrite growth from indium droplets or LIFT of (Cu,In,Ga) precursor layers are depicted in Fig. 1a) and b), respectively. The first approach (Fig. 1a)) starts from fs-laser roughened sites on molybdenum-coated glass substrates (1) into which indium assembles in the form of droplets upon physical vapor deposition (PVD) (2). These indium droplets are subsequently overcoated with cooper (3) and selenized, leading to chalcopyrite absorbers covered with copperselenides (4). After etching off the copperselenides by KCN solution, CISe micro absorber islands remain on the molybdenum back contact (5). In the second approach (Fig. 1b)), fs-laser pulses are utilized to locally transfer (Cu,In,Ga) precursor layers from a donor glass slide (1) onto a molybdenum-coated glass substrate (2). Upon selenization CIGSe micro absorbers form (3). Detailed process parameters for the various steps are given in the following.

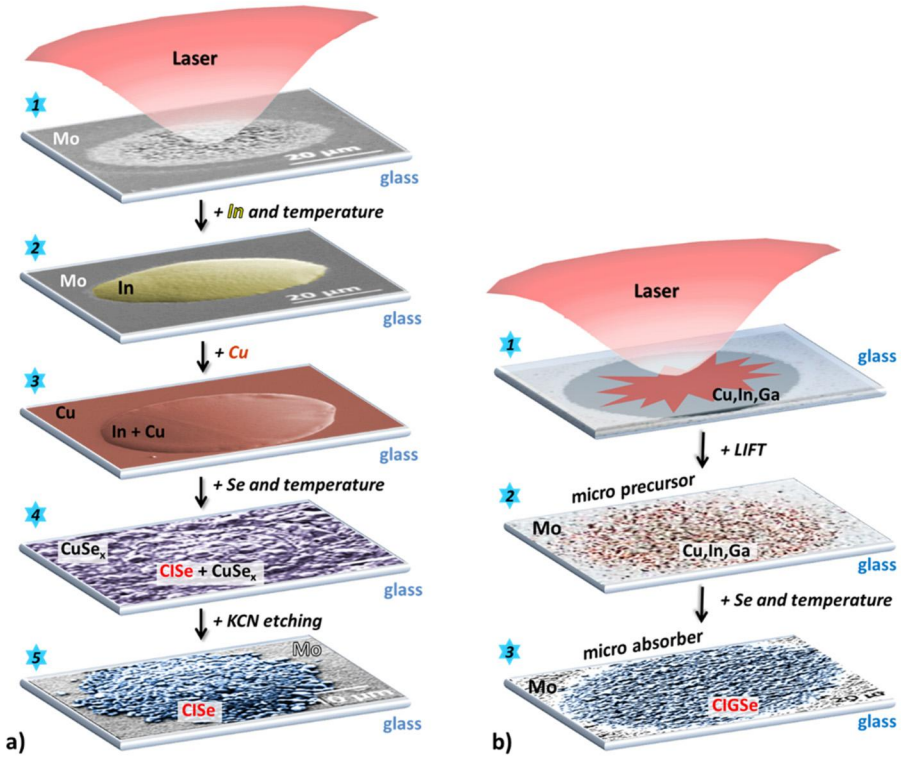

Figure 1. Process steps for local growth of chalcopyrite absorbers a) from indium droplets and b) by laser-induced forward transfer of (Cu,In,Ga) precursor layers.

2.1 Laser-patterning and indium (/gallium) deposition

Laser pulses of 30 fs duration and 790 nm wavelength were used to fabricate roughened sites on the surface of 2 mm thick glass substrates. Coating of the glass substrate with 100 nm thick molybdenum films was performed by PVD prior to or after laser-patterning [11].

For indium island growth, nominal 100 nm of indium were deposited by PVD at a rate of 0.3 Å/s and at a substrate temperature of 505 - 515°C. In the case of adding gallium, following the indium evaporation the substrate temperature was reduced to approx. 400°C and gallium of a nominal thickness of 30 nm was deposited at a rate of 0.15 Å/s.

2.2 Precursor preparation and corresponding laser-induced forward transfer

Copper, indium and gallium precursor layers were fabricated by E-beam (Cu) or thermal evaporation (In, Ga) at room temperature. The deposition rate for indium was 5 Å/s and for cooper 1 Å/s, whereas gallium was deposited via net weight. Thicknesses were varied from 10 - 150 nm for cooper and 150 - 1000 nm for indium and fixed at 100 nm for gallium. Donor substrates were coated with single layers, but a complete precursor layer consisting of a multi-layer stack of 30 nm Cu/200 nm In/30 nm Cu/90 nm Ga/30 nm Cu/ 200 nm In (from the glass side) was produced as well. As donor substrates served 150 µm thick glass slides.

For the laser-induced forward transfer, single laser pulses were applied which originated from the same Ti:sapphire fs-laser as used for laser patterning. Donor and acceptor substrate were separated by a distance of 150 µm with spacers. [12]

2.3 Selenization and solar cell fabrication

Selenization of local precursors was carried out at near-ambient pressure in a graphite box under addition of elemental selenium. The temperature profile included a 10 min alloying step at 200°C followed by a high temperature step of 550°C held for 6 minutes. This process was equally applied to cooper-coated indium droplets and to the LIFTed (Cu,In,Ga) micro precursors.

In the case of gallium-containing indium droplets, an alternative selenization process was chosen. Here, a selenium cracker source provided a temperature-controlled selenium flux to the UHV chamber into which the samples were placed. The temperature profile with respect to substrate temperature was: 30 minutes without heating, temperature increase at a rate of 30 K/min to 250°C, 12 minutes alloying phase and further increase by 30 K/min to the high temperature plateau (500 - 560°C), which was held for 6 minutes.

Electric separation of back and front contact in between individual micro absorbers, connected in parallel in a monolithic device, was achieved by spin-coating of SU-8 photoresist. Subsequently, a gentle reactive ion etching (RIE) step was applied to remove the uppermost part of the photoresist to uncover the top of the absorber islands for front contacting. Front contacts were formed by chemical bath deposition of 50 nm CdS and sputtering of 150 nm intrinsic and 230 nm Al-doped ZnO. Contact grids consisted of a Ni/Al bilayer.

2.4 Characterization

Structural characterization was carried out using an optical microscope or a scanning electron microscope (SEM) combined with energy-dispersive X-ray spectroscopy (EDX). Electrical characterization focused on measurements of current-voltage- (jV-) curves under standard test conditions (AAA sun simulator with AM1.5 spectrum) and in a concentrator sun simulator with light intensities varying from 1 to 100 suns.

3. RESULTS AND DISCUSSION

3.1 CISe and CIGSe micro absorber formation by island growth

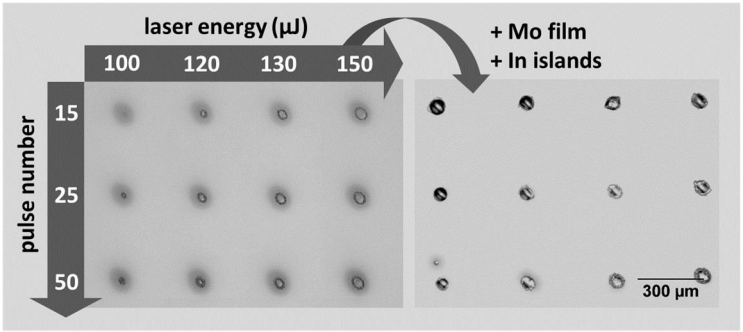

Figure 2. Optical micrographs of left: roughened sites on a glass substrate obtained by fs-laser pulses with varying pulse number and laser energy; right: laser-patterned glass substrate after coating with a molybdenum film (~100 nm thickness) and subsequent indium island growth at the roughened sites.

In the island growth approach, the most rare elements indium and gallium are economized by locally depositing droplets of In or (In,Ga) on laser-patterned sites. The laser-patterning of the substrate therefor constitutes the first essential step towards efficient selective growth. In Fig. 2 the influence of laser structuring parameters on the indium island growth is shown. The laser fluence was varied from 1.6 - 2.4 J/cm^{-2} (pulse energy of 100 µJ - 150 µJ) and the pulse number from 15 - 50. The resulting spot diameter of the roughened sites was between 25 and 70 µm (Fig. 2 left). After deposition of a thin molybdenum film and evaporation of indium, the islands preferentially assembled on the laser-patterned sites (Fig. 2 right). As it can be observed, within the entire parameter range indium islands nucleate on the laser spots. With the mildest laser parameters (top left spot) the substrate is only slightly roughened. The indium island growing on it corresponds morphologically to the islands that grow on an unstructured substrate. Their height and diameter are governed by the wetting properties of indium on molybdenum resulting in indium droplets. With an increase in the laser pulse energy or in the number of pulses the material ablation by the laser increases. Consequently, the surface is not only roughened, but also increasingly deep craters are formed. The morphology of the corresponding indium islands also changes: the islands become flatter (which is reflected in their brighter appearance under the light microscope) because their morphology increasingly resembles an indium "pond" that fills the laser craters only. Furthermore, also the evaporation conditions of indium (deposition rate, substrate temperature) influence the morphology of the indium islands, compare [13]. As optimum laser conditions fluences close to the modification (roughening) threshold and some tens of laser pulses per spot were identified.

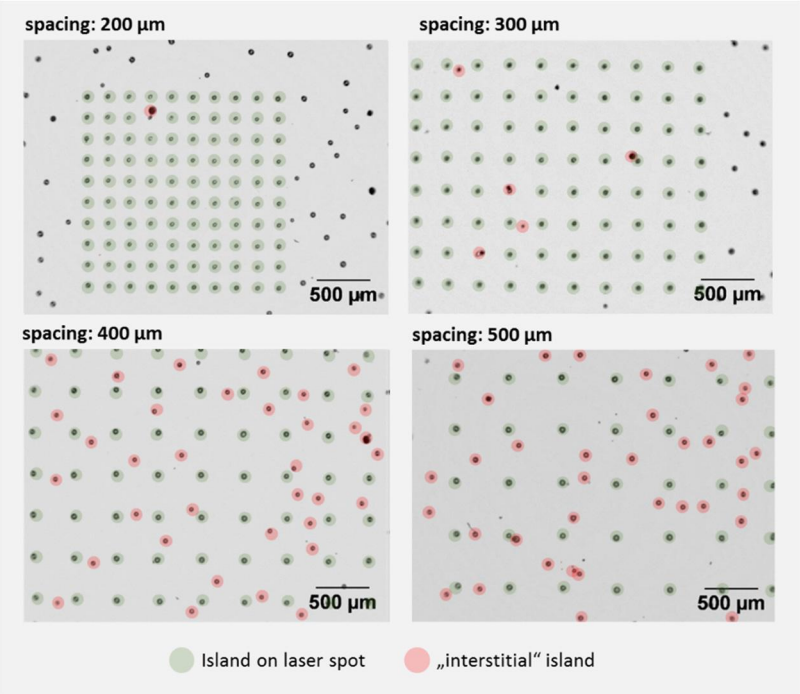

Figure 3. Influence of varying array spacing at constant indium island growth conditions (0.3 of Å/s deposition rate and 515°C substrate temperature); islands growing exactly on the laser roughened sites are marked in green, those occurring slightly or clearly off the pattern are depicted in red.

The flexibility in the local positioning of the laser-irradiated spots facilitates the adaptation of the indium island arrangement to the dimensions of micro lens arrays with which the micro absorbers are to be combined. With this respect, Fig. 3 investigates the influence of the array spacing on the selective indium island growth. Twenty pulses per spot each at an energy of 120 µJ were used for the fs-laser structuring of the glass substrate prior to the evaporation of molybdenum. Indium was deposited with a rate of 0.3Å/s at 515°C substrate temperature here. As the nearest neighbor distance (NND) of the freely growing islands under these conditions was in average 210 µm, the selective growth on laser patterns with 200 µm lateral spacing is most perfect. At 300 µm spacing, a few interstitial islands occur, but their number is still negligible for further application. If, however, the spacing distance is 400 µm or larger, the indium island growth is barely limited to the laser pattern and turns into a most random assembly. Yet, the growth in the patterned sites is maintained even at 500 µm spacing. In conclusion, it is essential to adjust the distances of the laser spots and the intrinsic NND of the islands (depending on the PVD parameters) to each another.

For the formation of CISe absorber material from the indium islands, a cooper layer with a thickness leading to an approximately stoichiometric Cu:In ratio needs to be added. In case of too low amounts of cooper, supplemental indiumselenides form, which hinder a pure absorber formation. However, for well-adjusted cooper layer thicknesses and indium island diameters, CISe absorbers can be produced revealing structural and opto-electronic material properties comparable to planar (film) references. For details of corresponding SEM/EDX and photoluminescence measurements, see [9].

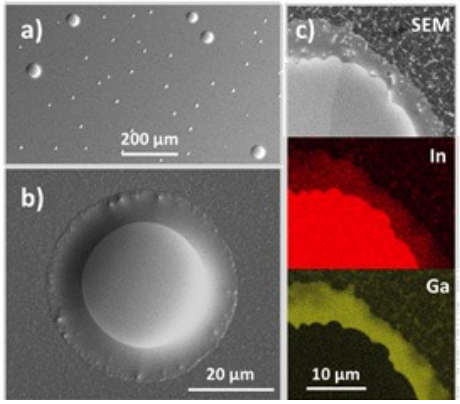

Figure 4. Growth of (In,Ga) droplets by sequential deposition of indium and gallium. a) and b) SEM images of (In,Ga) droplets, c) SEM image and corresponding EDX element maps of indium and gallium distribution at the edge of a droplet.

While indium assembles very well on the laser-patterned sites, given an adequate array spacing, local growth of gallium has emerged to be much more difficult to control. Due to the different melting and boiling points of indium and gallium, their different temperature dependence of surface mobility and adsorption-desorption equilibria, a sequential PVD process turned out necessary for the growth of (In,Ga) islands. Best growth conditions were obtained by depositing indium at a substrate temperature of ~ 500°C, followed by evaporation of gallium at ~ 400°C. Fig. 4 a) shows an SEM overview image of (In,Ga) precursor growth on a non-structured substrate. Gallium, deposited with a nominal thickness of 30 nm at a rate of 0.15 Å/s, aggregates preferentially at the existing indium islands; the small interstitial islands forming in addition are not expected to influence the performance of ordered, interconnected micro cells, since they are well separated from the main islands and comparatively small. Upon cooling down to room temperature, indium and gallium segregate in the precursor, as it can be deduced from Fig. 4 b) and c), which depict SEM and SEM/EDX measurements, respectively. At room, temperature, an indium rich core forms, which is surrounded by an annulus containing mainly gallium. This phase segregation is in line with the phase diagram of the eutectic In-Ga system, whose eutectic temperature is at about 15°C [14]. The annulus is liquid, which indicates, that during cooling solidification of almost pure indium starts in the center of the islands until the remaining liquid has reached an eutectic composition. The semi-stable structure of the annulus may originate from a thin galliumoxide surface layer.

For the subsequent selenization of these segregated (In,Ga) islands an improved intermixing of the elements was observed for increasing substrate temperatures, such that at 560°C CIGSe phases are found. Thin indium and in particular gallium wetting layers in between the islands can be removed by a mild RIE step before selenization to avoid shorting of the individual micro absorbers.

3.2 CIGSe absorber growth by LIFT approach

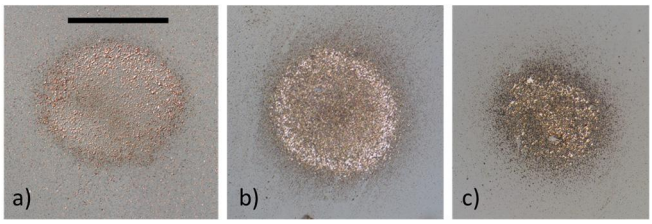

Figure 5. Result of laser-induced forward transfer of a) 20 nm Cu (2 J/cm^2), b) 150 nm In (5 J/cm^2) and c) 100 nm Ga (5 J/cm^2); the numbers in brackets indicate the laser fluence, the scale bar in the figure represents 100 µm.

The idea of utilizing laser-induced forward transfer for the local deposition of (Cu,In,Ga) precursors originates from previous successful application of the technique to various materials like metals, semiconductors or even biological tissue [15]. In a first attempt, layers of indium, gallium and cooper were transferred separately. The results are depicted in Fig. 5, revealing the transfer spots obtained for 20 nm Cu, 150 nm In and 100 nm Ga in a), b) and c), respectively. For all cases, a granular structure of the transferred material is observed, which is far from forming a compact micro spot. The influence of layer thickness as well as of peak laser fluences was tested for the donor films used for LIFT, in particular for indium and cooper, and an increase of required laser fluence with increasing film thickness found [12]. Yet, under none of the investigated conditions a compact material transfer could be achieved.

LIFT is initiated by vaporization of a thin slice of the donor layer at the boundary to the supporting glass. For metals the penetration depth of light into the layer is typically a few tens of nanometers, and with femtosecond laser pulses heat conduction is slow compared to other processes. These two conditions imply that the energy of the laser pulse is confined within the region defined by the penetration depth of the light, until vaporization starts. The vapor pressure propels the layer forward in the direction of the target. As it is the case for ablation, LIFT is a threshold driven process. Therefore, LIFT occurs only within an inner, encircled area of the laser beam cross section where the fluence is higher than the threshold value. For a circularly symmetric laser beam, this is the case for a disc-shaped area around the beam center and the boundary of the transferred material is shaped accordingly. Other mechanisms beside vaporization accompany LIFT, e.g. melting and other phase transitions as indicated by the formation of droplets during the process of material transfer. Reasoned by the confinement of laser energy close to the layer boundary, LIFT of a material stack appears a promising alternative to the transfer of individual materials. In this case, vaporization occurs mainly in the material closest to the supporting glass whereas the other material on top of it is not reached by the laser pulse. In particular, a thin cooper layer (20 nm, ~70% absorbed energy fraction) can act as a sacrificial layer for a most compact transfer of other thin metal films grown on top of it. Combining e.g. indium films with a thin sacrificial cooper layer resulted in successful compact transfer of the donor [12].

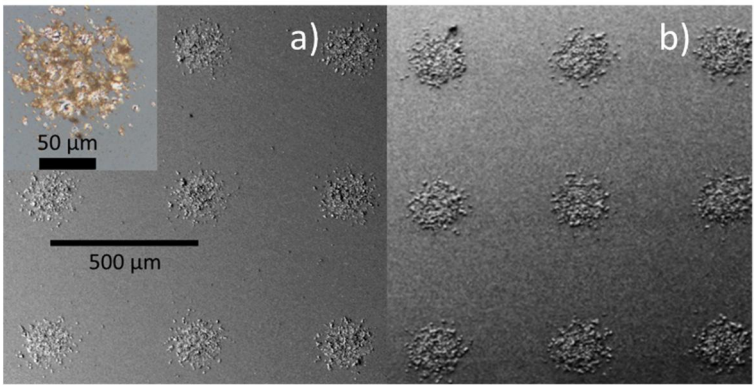

Fig. 6. SEM pictures of LIFTed (Cu,In,Ga) deposits on Mo/glass a) prior to and b) after selenization. The inset shows an optical micrograph of a (Cu,In,Ga) dot on the acceptor after the LIFT process (5 J/cm^2).

Based on the positive experiences with LIFT of bilayers, we then directly transferred discs from a (Cu,In,Ga) precursor stack. This stack was composed of 30 nm Cu/200 nm In/30 nm Cu/90 nm Ga/30 nm Cu/200 nm In, starting from the glass side. Fig. 6a) shows the local precursor dots on a molybdenum-coated glass substrate, resulting from illumination of the donor layer from the rear glass side with a single laser pulse of 5 J/cm^2 fluence. The observation from this SEM micrograph, and in particular from the optical microscope picture given as inset, is that material is deposited in clusters. However, upon selenization the growth of crystallites leads to a merging of clusters and therefore reasonably compact micro precursors with approx. 170 µm diameter (see Fig. 6b)). The resulting CIGSe micro absorbers still show a not perfectly homogeneous distribution of the elements indium and gallium and thus a spread of band gaps on the micro scale; yet, the averaged band gap corresponds well to good quality chalcopyrite material (for details see [10]). Furthermore, the micro absorbers benefit from the regular arrangement as defined by the lateral donor-acceptor alignment during the LIFT process.

3.3 Micro solar cell performance

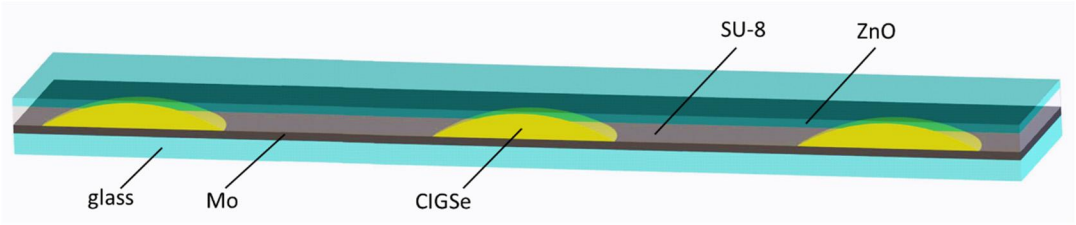

Figure 7. Schematic side view of CIGSe micro solar cells connected in parallel within a monolithic device; the micro absorbers with common back and front contact are electrically isolated by SU-8 photoresist.

Fig. 7 shows the schematic side view of CIGSe micro solar cells connected in parallel within a monolithic device. The micro absorbers were electrically isolated by spin-coating of SU-8 photoresist over the entire sample. A subsequent selective removal of the photoresist on top of the micro absorbers by a gentle RIE process allowed their contacting by a common Mo back and ZnO front contact. The combination of several micro absorbers to a micro solar cell device enables reaching sufficiently high currents that can be measured by opto-electronic characterization. The effective absorber area was estimated based on optical microscopy measurements in the case of nucleation samples and by calculations based on single dot diameter and array spacing for the LIFT approach, allowing for an estimation of current densities.

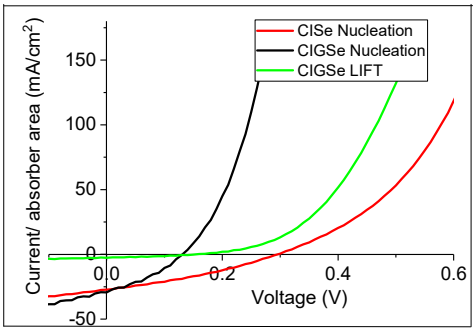

Figure 8. jV-characteristics (light measurements) of assemblies of CISe and CIGSe micro solar cells obtained by the island growth approach (labelled "Nucleation") and of CIGSe micro solar cells resulting from LIFT precursors.

The jV-characteristics of assemblies of typically 25 (LIFT) to 100 (nucleation) micro solar cells made from CISe and CIGSe fabricated by local growth (nucleation) from In and (In,Ga) islands, respectively, as well as from CIGSe grown from (Cu,In,Ga) precursors, deposited locally by LIFT, are compared in Fig. 8. Interestingly, the open circuit voltage of the CISe micro cells is higher than the one of the two types of CIGSe micro cells. This observation appears contradictory to the fact of increasing band gap energy with increasing gallium content. Yet, it may be explained by a still to be improved intermixing of indium and gallium in the quarternary compounds and hence a superior material quality of the CISe micro absorber. Furthermore, a significantly higher short circuit current density is observed for the absorbers fabricated by the island growth approach. Losses in current for the CIGSe micro solar cells fabricated by LIFT can e.g. be understood by the less compact growth of the absorber and resulting lower carrier generation and extraction. Overall, it has to be stressed that for all three fabrication approaches working micro solar cell devices could be achieved, which is remarkable given the fact that severe interventions to the standard growth processes were made.

The electric behavior of the three different types of micro solar cells is depicted in Fig. 9, where the main solar cell parameters short circuit current density j_{SC}, open circuit voltage V_{OC}, fill factor *FF* and efficiency are shown as a function of light concentration factor C (in suns). Contrary to the approach often used in literature, the light intensity was measured separately and not deduced from the current under the assumption of linear correlation. In this way we can investigate the dependence of the current on the concentration and observe that the linear behavior is indeed fulfilled by the CIGSe micro absorbers, yet not by the CISe absorbers (see Fig. 9a)). The deviation can be explained by the changes of series and shunt resistances - R_s and R_{sh} - as a function of light concentration. Whereas for the CIGSe micro absorbers R_s and R_{sh} drop similarly with increasing light intensity, R_s drops faster in the case of pure CISe (not shown). The deviation from linear rise of current reflects in the efficiency of the CISe micro solar cells, where a maximum is observed at 3 suns already (Fig. 9d)). This maximum also correlates with a drop in fill factor above 3 suns (compare Fig. 9c)), but would not have

been expected from the changes in V_{OC}. The open circuit voltage (plotted in Fig. 9b) on a logarithmic scale) initially experiences the expected logarithmic dependence on the concentration, but starts to drop at a concentration level between 10 and 100 suns. In combination with the maximum in *FF*, this determines the efficiency maximum for the CIGSe micro solar cells. Deviations from the theoretical V_{OC} behavior can be related to heating due to light concentration onto the entire substrate and not just onto the micro solar cells themselves. Thus, the maximum efficiency is reached for CIGSe solar cells fabricated by the nucleation growth approach, reaching 3.35% at 19 suns. The CISe micro solar cells achieve a similar value of 3.06% efficiency, however peaking already at 3 suns. If a linear increase of current with light concentration could be reassured here, an even better performance would be expected. Compared to these values, the efficiency of the LIFT CIGSe micro cells is about a factor of 10 smaller (maximum of 0.26% at 16 suns), originating basically from smaller current densities. Room for optimization is given and the agreement with general trends expected under light concentration makes further improvement promising.

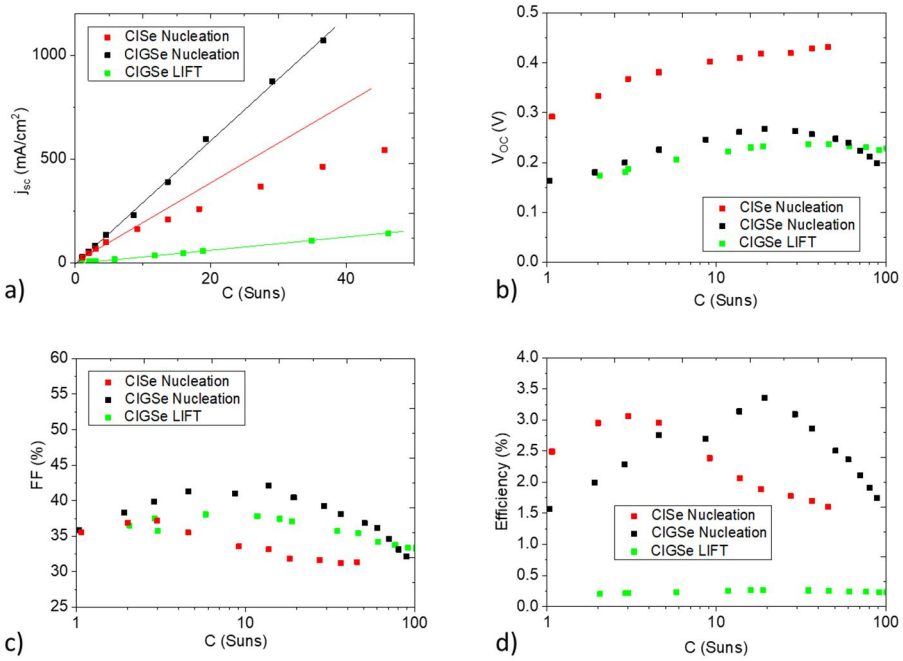

Figure 9. Development of solar cell parameters as a function of light concentration for CISe and CIGSe micro solar cells obtained by the nucleation approach and for CIGSe micro solar cells resulting from LIFT precursors: a) short circuit current density, b) open circuit voltage, c) fill factor and d) efficiency.

4. SUMMARY

In summary, we have demonstrated two novel bottom-up fabrication approaches for local growth of chalcopyrite micro solar cells leading to working devices, which show efficiency enhancement under light concentration. The first approach starts from site-selective growth of In or (In,Ga) droplets on fs-laser patterned substrates. Parameters like laser peak fluence and pulse number as well as pattern spacing are important for adequate growth of the indium islands. Intermixing of gallium with indium is a challenging task asking for further optimization. In the second approach of using laser-induced forward transfer for the fabrication of local precursor islands, the intermixing of cooper, indium and gallium is more homogeneous across the entire island, yet still subject to microscale variations which reflect in a to-be-improved quality of the transferred material. The method, however, benefits from the potential of simultaneous transfer of all precursor materials, facilitating the fabrication process. CISe and CIGSe micro absorbers obtained by the island growth approach as well as CIGSe micro absorbers fabricated via LIFT of (Cu,In,Ga) precursors were finalized to solar cell assemblies, which could be tested under 1 to 100 suns. Efficiency enhancement was proven for the presented technological approaches, reaching maxima at different concentration levels. A maximum at concentrations between 3 and 20 suns can be correlated to deviations from the expected linear increase in current or logarithmic rise of voltage as a function of light intensity. Related resistivity losses may be tackled by improved quality of absorber and isolating material, unwanted increase in temperature by application of micro lens arrays which will direct the incident light onto the micro solar cells only. The

combination with concentrator optics, which - asides further material optimization - constitutes the next step, will lead to an integrated device offering both material saving and efficiency enhancement.

ACKNOWLEDGMENT

The authors gratefully acknowledge financial support by the Deutsche Forschungsgemeinschaft (DFG) through BO 1129/6-1, KR 3638/3-1 and SCHM 2554/3-1. The research leading to these results has received funding from the European Union Seventh Framework Programme (FP7/2007-2013) under grant agreement nº 609788. B. Heidmann and M. Schmid are grateful to the Helmholtz Association for support from the Initiative and Networking Fund for the Young Investigator Group VH-NG-928.
The authors would like to thank M. Kirsch for ZnO sputtering and grid deposition and T. Köhler for support with the graphics of the paper.

REFERENCES

[1] "Renewables 2017 - Global Status Report", available at: http://www.ren21.net/gsr-2017/ (accessed: 21st December 2017).
[2] "Solar Frontier Achieves World Record Thin-Film Solar Cell Efficiency of 22.9%", available at: http://www.solar-frontier.com/eng/news/2017/1220_press.html (accessed: 21st December 2017).
[3] Paire, M., Lombez, L., Péré-Laperne, N., Collin, S., Pelouard, J.-L., Lincot, D., Guillemoles, J.-F., "Microscale solar cells for high concentration on polycrystalline Cu(In,Ga)Se_2 thin films," Appl. Phys. Lett. 98, 264102 (2011).
[4] Reinhold, B., Schmid, M., Greiner, D., Schüle, M., Kieven, D., Ennaoui, A., Lux-Steiner, M.Ch., "Monolithically interconnected lamellar Cu(In,Ga)Se_2 micro solar cells under full white light concentration," Prog. Photovoltaics Res. Appl. 23, 1929–1939 (2015).
[5] Lotter, E., Jackson, P., Paetel, S., "Identification of loss mechanisms in CIGS microcells for concentrator applications," Proc. 32nd EU-PVSEC, 1156–1160 (2016).
[6] Schmid, M., Yin, G., Song, M., Duan, S., Heidmann, B., Sancho-Martinez, D., Kämmer, S., Köhler, T., Manley, P., Lux-Steiner, M.Ch., "Concentrating light in Cu(In,Ga)Se_2 solar cells," Journal of Photonics for Energy 7, 018001 1-8 (2017).
[7] Duchatelet, A., Nguyen, K., Grand, P.-P., Lincot, D., Paire, M., "Self-aligned growth of thin film Cu(In,Ga)Se_2 solar cells on various micropatterns," Appl. Phys. Lett. 109, 253901 (2016).
[8] Sadewasser, S., Salomé, P.M.P., Rodriguez-Alvarez, H., "Materials efficient deposition and heat management of $CuInSe_2$ micro-concentrator solar cells," Sol. Energy Mater. Sol. Cells 159, 496–502 (2017).
[9] Heidmann, B., Ringleb, F., Eylers, K., Levcenco, S., Bonse, J., Krüger, J., Unold, T., Boeck, T., Lux-Steiner, M.Ch., "Local growth of $CuInSe_2$ micro solar cells for concentrator application," Mater. Today Energy 6, 238–247 (2017).
[10] Heidmann, B., Andree, S., Levcenko, S., Unold, T., Abou-Ras, D., Schäfer, N., Bonse, J., Krüger, J., Schmid, M., "Fabrication of regularly arranged chalcopyrite micro solar cells via femtosecond laser-induced forward transfer for concentrator application," ACS Appl. Energy Materials, DOI: 10.1021/acsaem.7b00028 (2017).
[11] Ringleb, F., Eylers, K., Teubner, Th., Boeck, T., Symietz, C., Bonse, J., Andree, S., Krüger, J., Heidmann, B., Schmid, M., Lux-Steiner, M.Ch., "Regularly arranged indium islands on glass/molybdenum substrates upon femtosecond laser and physical vapor deposition processing," Appl. Phys. Lett. 108, 111904 1-4 (2016).
[12] Andree, S., Heidmann, B., Ringleb, F., Eylers, K., Bonse, J., Boeck, T., Schmid, M., Krüger, J., "Production of precursors for micro-concentrator solar cells by femtosecond laser-induced forward transfer," Appl. Phys. A 123, 670 1-8 (2017).
[13] Ringleb, F., Eylers, K., Teubner, Th., Schramm, H.-P., Symietz, C., Bonse, J., Andree, S., Heidmann, B., Schmid, M., Krüger, J., Boeck, T., "Growth and shape of indium islands on molybdenum at micro-roughened spots created by femtosecond laser pulses," Appl. Surface Science 418, 548-553 (2017).
[14] Dickey, M.D., Chiechi, R.C., Larsen, R.J., Weiss, E.A., Weitz, D.A., Whitesides, G.M., "Eutectic gallium-indium (EGaIn): a liquid metal alloy for the formation of stable structures in microchannels at room temperature," Adv. Functional Materials 18, 1097–1104 (2008).
[15] Nagel, M., and Lippert, M., in "Nanomaterials: Processing and Characterization with Lasers," (ed. Singh, S.C., Zeng, H.B., Guo, C. and Cai, W.P.) Wiley (2012).